

***Ab initio* study of small vacancy complexes in beryllium**M. G. Ganchenkova^{1,*} and V. A. Borodin²¹*COMP/Laboratory of Physics, Helsinki University of Technology, P.O. Box 1100, 02015 Espoo, Finland*²*RRC Kurchatov Institute, Kurchatov Sq. 1, 123182 Moscow, Russia*

(Received 14 September 2006; revised manuscript received 12 December 2006; published 16 February 2007)

The paper presents the results of *ab initio* calculations of formation energies of vacancy and small vacancy complexes in beryllium. Particular attention is paid to the justification of the relevant computation parameters and the evaluation of the total and vacancy formation energy convergence. The vacancy formation energy of ~ 0.8 eV is predicted. The formation of divacancies from individual vacancies is found to be energetically unfavorable irrespective of the divacancy orientation in the lattice.

DOI: [10.1103/PhysRevB.75.054108](https://doi.org/10.1103/PhysRevB.75.054108)

PACS number(s): 61.72.Ji, 81.05.Bx

I. INTRODUCTION

Beryllium is one of the advanced materials for the application in future fusion reactors. In some concepts of forthcoming reactors Be is considered as the first wall material. Even more important may be the use of beryllium in a fusion reactor blanket with the aim of multiplication of neutrons from the $(n, 2n)$ reaction and the accompanying production of tritium, which is essentially the fusion reactor fuel. In all these applications the accumulation of big amounts of primary radiation defects (vacancies and self-interstitials) in irradiated metal is expected. Together with the nuclear transmutation products, first of all, helium and tritium, these primary defects can agglomerate into secondary defects (e.g., nanosized gas bubbles) that are known to cause at the macroscopic level such undesirable effects as swelling, embrittlement, and degradation of mechanical properties. In order to counteract these dangerous consequences of fast particle irradiation in real-life facilities, one needs a good understanding of the physical processes occurring in irradiated beryllium, which, in turn, requires the knowledge of basic properties of primary defects, such as their formation and migration energies, energies of defect interaction, etc.

Unfortunately, the database of the point defect parameters in beryllium is very scarce. Even the formation energy of vacancies is not known for certain. Sometimes 1.11 eV is cited as an experimental value for the vacancy formation energy (e.g., Ref. 1), but it is not clear whether this value was not actually introduced judging from beryllium cohesion energy. Alternatively, the vacancy formation energy can be estimated using the known values of self-diffusion activation energies (1.63 and 1.71 eV for out-of-plane and in-plane diffusion²) and the vacancy migration energy of 0.7–0.8 eV.³ Assuming the vacancy mechanism of self-diffusion, the vacancy formation energy should fall rather in the range of 0.8–1.0 eV. An alternative assessment based on the data of Ref. 4 (1.35 eV for self-diffusion energy and 0.65 eV for vacancy migration barrier) gives the vacancy formation energy of 0.7 eV, which is also noticeably less than the traditionally cited value.

In order to follow the kinetics of point defects, one needs to know more than the point defect formation energies. For example, in order to model the kinetics of vacancy clustering into voids (which at the macroscopic level is manifested as

the increase of material volume), one needs the interaction energies between vacancies in small clusters, starting from divacancies. At present, no measured data of this kind are available. In several papers^{1,5–7} the divacancy binding energies are estimated numerically using semiempirical potentials. The best of such potentials, those of modified embedded-atom (EAM) type,^{1,7} predict that the formation of divacancies is energetically favorable, even though the binding energy is relatively low (~ 0.2 eV). Unfortunately, qualitative estimates of defect parameters with the help of even the best semiempirical potentials are seldom completely trustworthy. At present much more reliable techniques are developed for these purposes, first of all, first-principles (*ab initio*) calculations based on the density-functional theory (DFT). However, while first-principles studies of the bulk beryllium properties are not rare (see, e.g., Refs. 8–10, and references therein), we are aware of only one paper¹¹ that estimates in this way the formation energy of monovacancy in Be. To the best of our knowledge, neither *ab initio* predictions of the divacancy interaction energies, nor other estimates of the vacancy formation energy, have been reported in the literature.

Here we present the results of DFT calculations for vacancies and small vacancy complexes in beryllium. The latter include three divacancies with physically nonequivalent orientations in the hexagonal-close-packed (hcp) beryllium lattice and two bigger cluster configurations, namely, a zig-zag trivacancy and an infinite vacancy chain in the prism direction. The latter two configurations were considered as possible nuclei of a unique defect observed during irradiation of beryllium—very narrow empty channels aligned along prism direction.^{12,13}

II. SIMULATION RESULTS

Our calculations have been performed using the VASP code¹⁴ with the generalized gradient approximation (GGA), which is known¹⁵ to describe the bulk and surface properties of beryllium better than the other widespread approximation for exchange-correlation energy, namely, the local-density approximation (LDA). The effect of core electrons was represented by ultrasoft Vanderbilt pseudopotentials implemented in VASP. During structural optimization, atoms were allowed to relax until the residual forces fell below

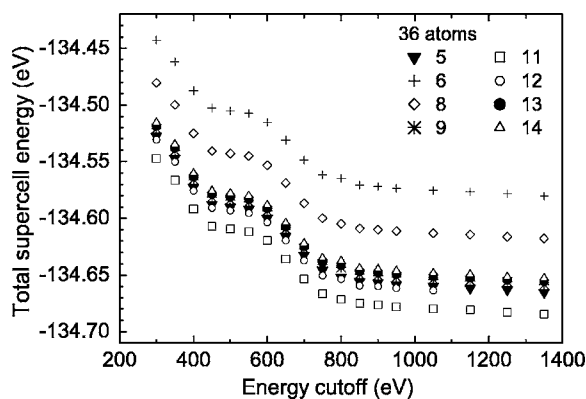


FIG. 1. The dependence of the total energy of the bulk 36-atomic supercell on cutoff energy for different densities (n, n, n) of k -point grids. Values of n corresponding to each particular curve are indicated in the legend.

0.01 eV/Å. Brillouin-zone sampling of the wave functions and charge density was done using the gamma-centered Monkhorst-Pack k -point grid.¹⁶

Due to the lack of earlier calculations of point defect properties, it was not *a priori* clear how big should be the simulation cell size, or how dense a sampling grid should be selected in order to guarantee the convergence of results. However, judging from the published studies of the bulk Be properties,¹⁰ it could be expected that quite dense k -point grids should be used. For this reason, we have performed first of all a thorough analysis of the total-energy convergence for the bulk Be lattice, using both LDA and GGA approximations.

Having in mind the necessity to simulate point defect properties, the size of the superlattice had to be selected sufficiently big in order to minimize the interaction of defects with their images imposed by periodic boundary conditions. On the other hand, the size of the computation cell had to allow calculations within reasonable time in spite of rather high computational resources required. As a reasonable compromise, we have selected a $4 \times 4 \times 3$ (96-atomic) supercell as a basic one for this study. In addition, we have thoroughly studied a supercell consisting of $3 \times 3 \times 2$ (36 atoms) elementary cells in order to get a database for comparison with the earlier calculations for a monovacancy,¹¹ though even for a monovacancy such a cell is insufficient in order to completely avoid the influence of the defect images caused by periodic boundary conditions. Finally, in order to estimate the convergence of results with the cell size increase, a number of calculations were performed for 128- and 200-atomic supercells ($4 \times 4 \times 4$ and $5 \times 5 \times 4$ elementary cells), but these were restricted to monovacancy only, because accurate simulations of beryllium behavior are quite demanding in terms of computation resources.

Indeed, for both 36-atomic (as shown in Fig. 1) and 96-atomic supercells we have found that the energy cutoff of ~ 900 eV and a high number of k points [at least (12,12,12) sampling mesh] are required to reach the total-energy convergence of the bulk lattice. Note that the recent calculations of the bulk beryllium properties¹⁵ also employ a dense k -point mesh. In compliance with the earlier results,¹⁵ it has

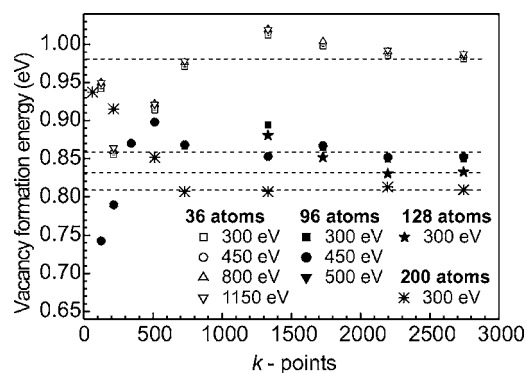


FIG. 2. The dependence of the vacancy formation energy on the number of points in the k -point grid at different cutoff energies (as indicated in the legend). The supercell sizes and cutoff energies are summarized in the legend. The dashed lines indicate the converged levels of formation energies for different supercell sizes.

been found that GGA reproduces the experimental equilibrium lattice parameters somewhat better than LDA and so only GGA was used below to determine the defect properties.

In order to specify the supercell edge lengths, the bulk lattice energy of the supercell was minimized with respect to both basal (in-plane) and prism lattice parameters, denoted below a and c , respectively. The optimized total energy $E_t = -3.73$ eV/atom was reached at parameter values $a = 2.259$ Å and $c/a = 1.572$, which are in reasonable agreement with the experimental ones [$a = 2.286$ Å and $c/a = 1.568$ (Ref. 17)]. These values of lattice parameters were used in all subsequent calculations of defects, where no further supercell size relaxation was allowed. The total energy in the vicinity of the optimized lattice parameters could be excellently fitted by a parabolic function of c and a , while the curvature of the fitting function in the minimum of the total crystal energy allowed us to estimate the elastic constants (in Voigt's notation) as $C_{11} + C_{12} = 294$ GPa, $C_{13} = 27.9$ GPa, and $C_{33} = 389$ GPa, in reasonable agreement with both the experimental data, $C_{11} + C_{12} = 300 - 320$ GPa, $C_{13} = 5 - 14$ GPa, and $C_{33} = 340 - 370$ GPa (see Ref. 18, and references therein), and the earlier computer estimates (summarized, e.g., in Ref. 15). The cohesive energy, determined as the difference between the optimized total energy per atom and the energy of one Be atom in vacuum, was found to be -3.70 eV/atom, which agrees well with the numerical estimates for similar calculation conditions¹⁵ and is in reasonable agreement with the experimental value of -3.32 eV.¹⁹

Like in the bulk lattice case, the total-energy convergence was checked during the relaxation of supercells with vacancy defects. The general behavior of the total energy as a function of the cutoff energy follows closely that shown in Fig. 1 for the bulk crystal. However, the monovacancy formation energies practically cease varying for cutoff energies above ~ 600 eV. At lower cutoff energies (from 300 to 600 eV) a steady increase of the vacancy formation energy with the increase of the cutoff energy is observed, but for both 36- and 96-atomic cells this increase did not exceed 0.01 eV (see Fig. 2), and it may be expected that, quite generally, the use of the cutoff energy of 300 eV only slightly underestimates

TABLE I. The *ab initio* predictions of the vacancy formation energy in beryllium for different supercell sizes, in comparison with the literature data.

Supercell size	E_V^f , eV
36 atoms	0.98
96 atoms	0.86
128 atoms	0.83
200 atoms	0.81
Earlier predictions	
<i>Ab initio</i> (Ref. 11)	1.12
EAM (Ref. 7)	1.12
EAM (Ref. 6)	1.13
EAM (Ref. 1)	1.23

the defect formation energy. On the other hand, the sensitivity of the vacancy formation energy to the choice of k -point sampling density is only slightly decreasing with the growth of the supercell size and in order to reach a good convergence (within ± 0.01 eV), at least an (11,11,11) sampling mesh is required even for the biggest considered supercell. As can be seen in Fig. 2, if the convergence is not achieved, the deviations from the converged values can reach 0.2 eV and be of any sign.

The best converged estimates of the vacancy formation energy E_V^f for different used supercell sizes are summarized in Table I (the latter includes also the earlier calculation predictions from both *ab initio* and EAM calculations). As can be seen, the values obtained here are close to the numbers derived from the known experimental data (see the Introduction), but are noticeably less than the earlier predictions. The latter is not very surprising as far as the semiempirical potentials are concerned. Even though all of these consistently give values above 1.1 eV, such consistency for pronouncedly different many-body potentials results largely from the fact that the potential parametrizations oriented at the value of 1.11 eV, assumed to be the experimental vacancy formation energy. Much less clear is the discrepancy between the present results and the value of 1.12 eV predicted by the earlier *ab initio* calculations.¹¹ Even in the 36-atomic cell, as used by Krimmel and Fähnle,¹¹ we get for the vacancy formation energy the converged value of 0.98 eV, which is much closer to our results for the bigger cells. Possibly, the reason for the remaining difference should be ascribed to the insufficient amount of k points in Ref. 11 (which was, unfortunately, not stated explicitly) and/or to the use of LDA approximation, which, as we have already mentioned, gives somewhat worse predictions for Be than GGA.

As can be seen in Fig. 3, the vacancy formation energy decreases noticeably when coming from 36 to 96 atoms per cell, but the subsequent supercell size increase changes the vacancy formation energy only moderately. The energy decrease as a function of the cell volume can be nicely fitted by a power law with the exponent of -1 . If this trend holds true for higher supercell sizes, the vacancy formation energy would tend to ~ 0.78 eV as the cell volume tends to infinity.

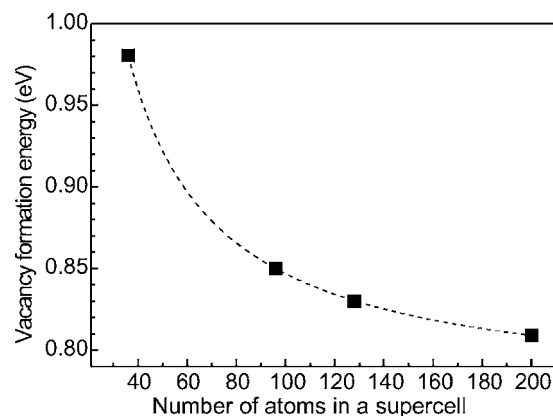


FIG. 3. The monovacancy formation energy as a function of the supercell size [all values are for energy cutoff 300 eV and (14,14,14) k -point mesh]. Dashed line shows a power law fit.

The good convergence of the vacancy formation energy with the supercell size is most probably due to the fact that the vacancy dilatation in Be is small, so that the effect of the vacancy elastic interaction with its periodic images is not pronounced.

The relaxation pattern around a vacancy is shown in Fig. 4(a). Six atoms in the basal plane, located at the first-nearest-neighbor separation from the vacant site, shift towards the vacancy by less than 0.2%, while the shape of the hexagon formed by these atoms slightly distorts. The triangles of the first-nearest-neighbor atoms lying in the basal planes above and below the vacancy stay practically within their planes and remain perfectly equilateral, but the distances between the atoms shrink by approximately 1%. The overall lattice relaxation around a vacancy is very small, especially in comparison to fcc and bcc metals, where the vacancy dilatation is typically $\sim -20\%$.²⁰ Such low elastic relaxation is consistent with both the earlier *ab initio* predictions¹¹ and the results of EAM-based calculations.

In addition to monovacancy, we have studied three divacancy configurations, as shown in Figs. 5(a)–5(c), namely, in-plane and out-of-plane vacancy pairs at the first-nearest-neighbor (1NN) separation (denoted as $2V_{aa}$ and $2V_{ac}$, respectively) and a vacancy pair at the 3NN separation, aligned along the c axis ($2V_{cc}$). The effect of the k -point grid density on the divacancy formation and binding energies, E_{2V}^f and E_{2V}^b , is demonstrated in Table II. The binding energy for divacancies is defined as the energy gain from putting together two separate vacancies, $E_{2V}^b = 2E_V^f - E_{2V}^f$. It is seen that sufficiently dense k -point grids provide the good convergence of results.

Like in the monovacancy case, the elastic relaxation of atoms surrounding divacancies is very low, but the symmetries of relaxation patterns are more complicated and depend very much on the divacancy orientation. The simplest situation is met for $2V_{cc}$, where the relaxation pattern around each vacancy in the pair practically replicates that for a monovacancy, as shown in Fig. 4(a). For the in-plane divacancy $2V_{aa}$, the relaxation of the neighbor atoms surrounding the vacancy pair in the same basal plane shows a low-symmetry pattern with some bond lengths changing up to 3%, while the

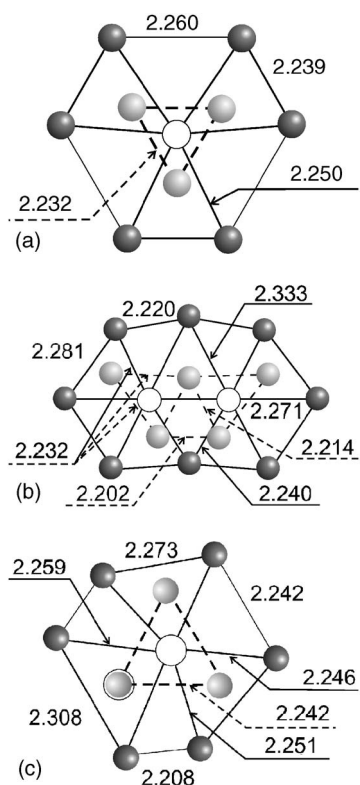


FIG. 4. Atomic relaxation pattern around a vacancy (a), divacancy $2V_{aa}$ (b) and divacancy $2V_{ac}$ (c). The numbers in the figure indicate the distances between corresponding neighbor atoms in Å. Dark spheres represent atoms in the vacancy basal plane, light spheres—in the adjacent basal planes. In (c) the relaxation only around one vacancy is shown, the relaxation around the other one (visible as a circle under the left bottom light sphere) is symmetric. Distortions of the atomic configurations around the defects are largely exaggerated in order to clearly illustrate the relaxation symmetry.

neighbors in the adjacent basal planes somewhat rearrange, but remain practically in their own planes, Fig. 4(b). The modification of the short-range environment symmetry for the out-of-plane divacancy, $2V_{ac}$, is shown in Fig. 4(c).

The converged divacancy formation and binding energies are summarized and compared with the earlier predictions in Table II. The discrepancy between the current estimates of the divacancy formation energies and those by EAM potentials (e.g., Ref. 6) is quite pronounced. On the contrary, the divacancy formation energies predicted by MEAM potentials are reasonably close to *ab initio* values. However, *ab initio*

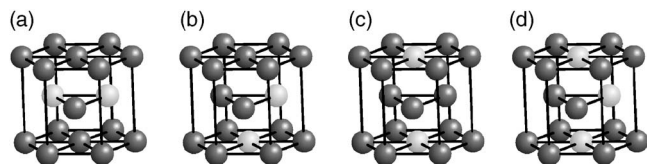


FIG. 5. The configurations of considered vacancy clusters: (a) divacancy $2V_{aa}$, (b) divacancy $2V_{ac}$, (c) divacancy $2V_{aa}$, and (d) trivacancy $3V_{cac}$ in beryllium lattice. Dark spheres represent Be atoms, light spheres are vacant sites.

TABLE II. Small vacancy cluster formation and binding energies in 96-atomic cell for different densities of the k -point grid and 300-eV energy cutoff. For comparison, the literature data are included, where available.

Configuration	k points	E_{2V}^f , eV	E_{2V}^b , eV
$2V_{aa}$	$11 \times 11 \times 11$	2.00	-0.21
	$12 \times 12 \times 12$	1.97	-0.24
	$13 \times 13 \times 13$	1.96	-0.26
	$14 \times 14 \times 14$	1.96	-0.26
Earlier predictions			
	EAM (Ref. 7)	2.09	0.15
	EAM (Ref. 6)	1.58	0.68
	EAM (Ref. 1)	2.29	0.17
$2V_{ac}$	$11 \times 11 \times 11$	2.09	-0.36
	$12 \times 12 \times 12$	2.11	-0.32
	$13 \times 13 \times 13$	2.08	-0.35
	$14 \times 14 \times 14$	2.07	-0.37
Earlier predictions			
	EAM (Ref. 7)	2.11	0.13
	EAM (Ref. 6)	1.51	0.75
	EAM (Ref. 1)	2.25	0.21
$2V_{cc}$	$11 \times 11 \times 11$	2.00	-0.21
	$12 \times 12 \times 12$	1.97	-0.24
	$13 \times 13 \times 13$	1.96	-0.27
	$14 \times 14 \times 14$	1.97	-0.27
$3V_{cac}$		7.08	-0.35 ^a
c chain		7.40	-0.36 ^b

^aEstimate for the binding between monovacancy and $2V_{ac}$ divacancy.

^bEnergy gain per vacancy.

and semiempirical predictions are qualitatively different, where the divacancy binding energies are concerned. Due to the fact that vacancy formation energy is found to be lower than usually assumed, the agglomeration of individual vacancies into divacancies is energetically unfavorable. We have checked that the increase of the cell size to 200 atoms practically does not change the binding energy values, though a systematic search for converged numbers for the binding energies in this case was not attempted due to prohibitively high computational costs.

The unfavorability of vacancy binding is a matter of principle for the predictions of vacancy clustering kinetics in beryllium. Indeed, positive vacancy binding, as expected from semiempirical estimates, means a possibility of pure void swelling of beryllium. The fact that the divacancy binding is relatively weak (at the level of 0.2 eV) means only that the range of experimental parameters (temperatures, point defect generation rates) required for void swelling observation can be rather narrow. A similar situation is met in the case of pure iron and ferritic steels, which are able to swell (e.g., Ref. 21), even though the divacancy binding energies in iron are of approximately the same magnitude.²² On the

contrary, the energy penalty for the divacancy formation means in practice that the void swelling of beryllium is completely suppressed, unless, naturally, the crystal contains impurities (e.g., gas atoms) that stabilize vacancy clusters.

Indeed, when divacancy formation is suppressed, chances for the formation of bigger vacancy clusters become negligible, even if these bigger clusters were energetically favorable. However, the latter also does not seem to be the case in beryllium, as can be judged from our calculations for a trivacancy [denoted as $3V_{cac}$ and shown in Fig. 5(d)] and a zigzag chain of vacancies in the prism direction (c -chain). Within one elementary cell the latter defect looks as in Fig. 5(d), but it runs through the whole simulation cell and includes six vacancies in a 96-atomic cell; having in mind periodic boundary conditions, this defect represents an infinite chain along the c axis. As can be seen in Table II, an addition of one more vacancy to a $2V_{ac}$ divacancy is as energetically unfavorable, as the formation of the divacancy itself. The formation of a c -chain from six individual vacancies also requires additional energy of ~ 0.36 eV per vacancy. This means that the formation of experimentally observed thin open channels, like the formation of more common 3D cavities, is most probably promoted by gaseous impurities, introduced in Be samples during implantation.

The inherent stability of beryllium against void formation means that one should expect no void swelling in pure beryllium irradiated with electrons in the 1–2 MeV range, which produce point defects but do not contaminate the samples with undesirable impurities. Unfortunately, this conclusion is not easy to verify, because the reported swelling

measurements in beryllium have been done under neutron irradiation in nuclear reactors.^{23,24} They generally report quite low swelling of irradiation beryllium, but do not allow us to completely exclude the effect of nuclear transmutation products (helium and tritium atoms), that are known to efficiently promote bubble formation.^{12,13,25}

III. CONCLUSIONS

In this paper the formation energies of vacancies, divacancies, and some other small vacancy clusters in hcp beryllium have been estimated using first-principles quantum-mechanical simulations. It has been found that the energy of vacancy formation is close to 0.8 eV, which is less than predicted by the earlier numerical simulations, but falls in the range expected from the available experimental data. In contrast to the earlier calculations based on semiempirical potentials, it has been demonstrated that the formation of divacancies and other considered small vacancy complexes from individual vacancies is energetically unfavorable, which can be a microstructural reason for the high resistance of Be to void swelling.

ACKNOWLEDGMENTS

This research has been supported by the Academy of Finland through the Centers of Excellence program (2006–2011). We also wish to thank the Center for Scientific Computing (Helsinki, Finland) for the use of their computational facilities.

*Electronic address: mgc@fyslab.hut.fi

¹M. I. Baskes and R. A. Johnson, *Modell. Simul. Mater. Sci. Eng.* **2**, 147 (1994).
²Y. Adda and J. Philibert, *La Diffusion Dans les Solides* (Presses Universitaires De France, Paris, 1966), Vol. II, p. 1132.
³J. C. Nicoud, J. Delaplace, J. Hillairet, D. Schumacher, and Y. Adda, *J. Nucl. Mater.* **27**, 147 (1968).
⁴Y. Chabre, *J. Phys. F: Met. Phys.* **4**, 626 (1974).
⁵M. Igarashi, K. Khantha, and V. Vitek, *Philos. Mag. B* **63**, 603 (1991).
⁶J.-M. Cayphas, M. Hou, and L. Coheur, *J. Nucl. Mater.* **246**, 171 (1997).
⁷W. Hu, B. Zhang, B. Huang, F. Gao, and D. J. Bacon, *J. Phys.: Condens. Matter* **13**, 1193 (2001).
⁸U. Häussermann and S. I. Simak, *Phys. Rev. B* **64**, 245114 (2001).
⁹G. V. Sin'ko and N. A. Smirnov, *Phys. Rev. B* **71**, 214108 (2005).
¹⁰G. Robert and A. Sollier, *J. Phys. IV* **134**, 25 (2006).
¹¹H. Krimmel and M. Fähnle, *J. Nucl. Mater.* **255**, 72 (1998).
¹²N. Yoshida, S. Mizusawa, R. Sakamoto, and T. Muroga, *J. Nucl. Mater.* **233-237**, 874 (1996).

¹³V. N. Chernikov, V. Kh. Alimov, A. V. Markin, and A. P. Zakharov, *J. Nucl. Mater.* **228**, 47 (1996).
¹⁴G. Kresse and J. Hafner, *Phys. Rev. B* **47**, 558 (1993); G. Kresse and J. Furthmüller, *Phys. Rev. B* **54**, 11169 (1996).
¹⁵N. A. W. Holzwarth and Y. Zeng, *Phys. Rev. B* **51**, 13653 (1995).
¹⁶H. J. Monkhorst and J. D. Pack, *Phys. Rev. B* **13**, 5188 (1976).
¹⁷C. S. Barrett and T. B. Massalski, *Structure of Metals*, 3rd ed. (Pergamon, Oxford, 1980).
¹⁸A. Migliori, H. Ledbetter, D. J. Thoma, and T. W. Darling, *J. Appl. Phys.* **95**, 2436 (2004).
¹⁹C. Kittel, *Introduction to Solid State Physics* (Wiley, New York, 1976).
²⁰H. Wollenberger, in *Physical Metallurgy*, 3rd ed. (North-Holland, Amsterdam, 1983), Vol. 3, p. 1140.
²¹F. A. Garner, M. B. Toloczko, and B. H. Sencer, *J. Nucl. Mater.* **276**, 123 (2000).
²²C. Domain and C. S. Becquart, *Phys. Rev. B* **65**, 024103 (2001).
²³V. P. Chakin, V. A. Kazakov, R. R. Melder, Yu. D. Goncharenko, and I. B. Kupriyanov, *J. Nucl. Mater.* **307-311**, 647 (2002).
²⁴L. L. Snead, *J. Nucl. Mater.* **326**, 114 (2004).
²⁵R. A. Causey, *J. Nucl. Mater.* **300**, 91 (2002).